ENGINEERING TRANSACTIONS • *Engng. Trans.* • **65**, 1, 133–145, 2017
Polish Academy of Sciences • Institute of Fundamental Technological Research (IPPT PAN)
National Engineering School of Metz (ENIM) • Poznan University of Technology

Modelling of Damping Properties of Articular Cartilage During Impact Load

Tomasz KLEKIEL[1)], Jakub WODZISŁAWSKI[2)], Romuald BĘDZIŃSKI[1)]

[1)] *University of Zielona Góra*
Licealna 9, 65-419 Zielona Góra, Poland
e-mail: t.klekiel@ibem.uz.zgora.pl

[2)] *Military Clinical Hospital*
Borowska 213, 50-556 Wrocław, Poland
e-mail: jakub.wodz@gmail.com

The paper presents some details about difficulties in modelling of articular cartilage. The most useful method to simulate a mechanism of tissue deformation during load is Finite Element Method (FEM). In this paper the authors present an approach of modelling a damping phenomenon in articular cartilage of an ankle joint. The damping property was modelled and analysed with an assumption that the reaction force is different suitable to change of a dynamic load. The model of lower extremity consists of three main bones: tibia, fibula and talus. The force acting on the model was generated from displacement of the talus according to the main biomechanical axis of a leg. The results present the role of an articular cartilage in distribution of energy inside the lower extremity. The analysis was carried out according to three main aspects: the reaction force in a support, the influence contact on the energy dissipation and the role of cartilage thickness in transmission of energy by the tibiotalar joint.

Key words: biomechanics, ankle joint, cartilage, stresses in cartilage, damping, finite element.

1. Introduction

Articular cartilage lesions are not usually healed. The healing is possible only under special biologically conditions [1]. The knowledge of hyaline articular cartilage contact deformation is important to understand the function and ethology of osteopathists [2]. The deformation of cartilage is shown as the change of the contact area. During static loading this deformation is formed within a couple of seconds.

One of the cartilage models is the two-phase model proposed by the Mow [3]. This model assumes that the cartilage is a mixture of two elements of solid and fluid materials. 75% of all ankle injuries are ankle sprains and 25% of those injuries are caused by the impact load such as running, jumping and etc. [4]. The force is propagated from a foot to the neighbouring bones by an ankle joint that the thickness of cartilage is about only 1.4 to 2.0 mm [5].

The Finite Element Method (FEM) can be used to determine the contact forces, deformations and calculations of strain energy [6]. The significant problem is focused on material properties for cartilage. Typically in dynamic problems the cartilage is modelled as an isotropic linear or a visco-elastic model [7]. FEM allows defining a constitutive model of material, including nonlinear characteristics [8]. Many experimental studies confirm visco-elastic properties of the cartilage [9]. The Articular cartilage plays a major role in damping vibrations and dissipating energy as a result of impact loads [10]. Nowadays, there is no a sufficiently good model describing the complex properties of a cartilage.

An ankle is a very complicated joint with the main contact of cartilages between tibia and talus. According to this connection the energy is transmitted between the base of a foot and a body in both directions. During static load the reaction force is equally loaded. For a dynamic problem the reaction force is different and depends on the time. The maximum force value is less than the peak of the force acting on the model. The particular structures like bones, ligaments and cartilages work on a dissipation of energy inside an extremity. In an experimental study on dynamic systems damping is measured based on a reaction force in the support during impact loading [11–13].

This work is focused on the analysis of tibiotalar joint. The numerical model consists of the function and the geometry of an articular cartilage [5]. The investigation of a cartilage deformation under the impact load was carried out based on the model containing tibia, fibula and talus. These bones are connected by the cartilage layers. The geometry model of joint was received from MRI image data. The bone structure was defined as the isotropy material with the division on a cortical and a trabecular bone. This assumption was dictated by the time consumption during calculation. The bone model consists of trabecular and cortical layers and it is usually used in numerical investigations [14]. These models with an approximate thickness of cortical layer are characterized by the stiffness of structure on the outside. Inside the structure it is more flexible. During the effort of a bone the outside layers have higher stresses what is similar to natural phenomena because it is protecting mechanism for vessels inside a bone. The articular cartilage was modelled by flexible finite elements with different material properties.

2. Material and methods

The articular cartilage is composed of solid and fluid phases. The interaction of these determines the mechanical property. The fluid phase consists of the water over 75% of all weight [15]. The solid phase is composed of chondrocytes, collagen fibers, proteoglycans, lipids and glycoproteins. The cartilage can be separated by four main zones: the superficial, the middle, the deep and the calcified [15]. From the outside approximately 15% of full thickness is a superficial zone which contains collagen fibers oriented in the direction of shear stress. Next layer consists collagen fibers oriented perpendicular to the contact layer. The maximal ultimate stress is defined along the fibers similar to composite material [16]. In numerical investigations this complicated structure is usually approximate to an isotropic or a visco-elastic material model with parameters selecting from an experimental study [17, 18].

2.1. Model of lower extremity

The behaviour of articular cartilage was analysed by the model with consists three main bones: tibia, fibula and talus. These three bones make up the ankle joint with contact layers in C shape [19]. The bones in the considering model are prepared with a high quality. In result, it is possible to analyse any changes in these structures and the influence of cartilage characteristics on the reaction in all bones.

The experimental investigations focused on the problem of transmission energy in lower extremity are realized based on cadavers or human dummy [11, 20–22]. The problem is analysed by measurement of reaction forces during loading. The energy transmission is controlled with an assumption that the leg is supported in one end of a leg and the second end is loaded by a force from an accelerated mass. The same solution was used to control the energy transmission in a numerical model. The proximal head of tibia is supported in a place of cartilage. The load force is generated form the movement of talus along the main axis of tibia. The tibiotalar joint (Fig. 1a) consists of the cartilages on tibia, fibula and talus (Fig. 1c). Between these cartilages, the synovial capsule is defined. Between tibia and fibula the cartilage is defined such as on (Fig. 1b). All bones are defined as the layer with a cortical and trabecular bone phase.

The mechanical properties of the bones are defined based on the data from other previous study [14, 19]. The cortical bone in the tibia and fibula was Young's modulus equal 18e3 MPa and Poission's ratio was equal 0.3. For the talus cortical bone the Young's modulus was defined as 17e3 MPa and Poisson's ratio 0.3. The trabecular bone space (Fig. 2, elements 1 and 2) was defined as isotropic material with Young's modulus 700 MPa and Poisson's ratio 0.3 [14]. The model consists also ligaments which were defined as a spring object for stabilization of the ankle. The stiffness for ligaments was determined based on data presented by Ramlee *et al.* [22].

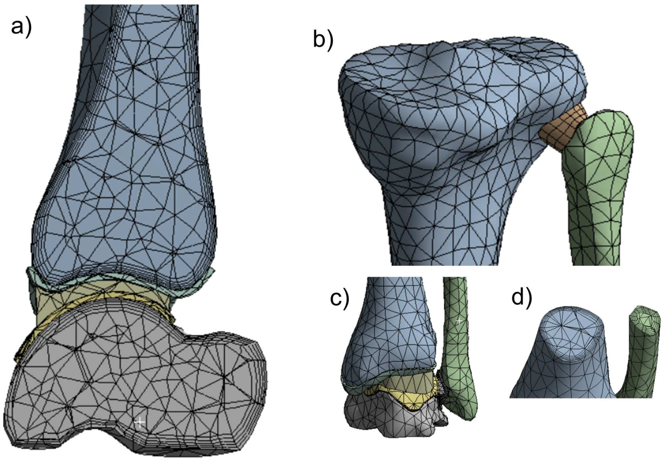

Fig. 1. Details about model.

2.2. *Properties of tibiotalar joint*

The articular cartilage is composed of proteoglikans, fiber net of collagen and elastin and fluid in quantity of 70–85% of cartilage weight [15]. This structure is highly deformable which allows increasing the contact area adapted to loading [3].

The shape of the articular cartilage in an ankle was prepared from MRI image data [21]. The thickness of a cartilage in different places was measured using the software 3D DOCTOR. Based on these data the shape of a cartilage on the respective bones was modelled in SOLIDWORKS. The MRI data was affected to 30 years old man with a healthy ankle joint. The measurement results were compared to the data published by Millington [23]. The Fig. 2 presents the

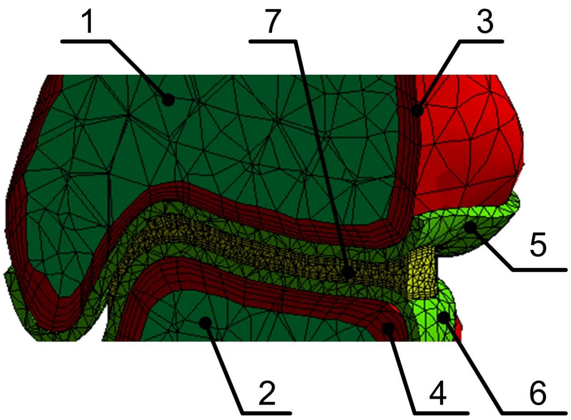

Fig. 2. The model of cartilage: 1 – trabecular bone for the tibia, 2 – trabecular bone for the talus, 3 – cortical bone for the tibia, 4 – cortical bone for the talus, 5 – Cartilage layer for the tibia, 6 – Cartilage layer for the talus, 7 – synovial capsule.

results of cartilage modelling. The individual layers of trabecular and cortical bones, cartilages and synovial capsule were represented in the model by finite elements with different material properties. For the healthy cartilage the distance between bones must be in the range of 4–5 mm [4]. The shape of synovial capsule was modelled based on a mean contact area between tibia and talus with a typical change under load [2].

The behaviour of the articular cartilage in ankle joint was modelled by the Venturato *et al.* [26]. The constitutive model of cartilage was proposed for characterization the multiphase structure. In our case, the properties for synovial capsule were assumed similar to Venturato model. The Young's modulus was equal $E = 6$ MPa and Poisson's ratio 0.45 [27].

The Table 1 includes parameters for six selected models of cartilage structure. First case is applied to the isotropic model of cartilage with properties proposed by Danso [24]. This model assumed large stiffness of cartilage by the high value of Young's modulus. According to work realized by Ozen *et al.* [28], the articular cartilage was defined as the isotropic material with Young's modulus equal 10 MPa. In the model proposed by Niu [12] the cartilage component has Young's modulus equal only 1 MPa.

Table 1. The parameters of articular cartilage model.

No	Model name	Parameters	Ref.
1	linear	$E = 93$ MPa, $v = 0.3$	[24]
2	Neo-Hookean (*)	$c_1 = 30$ [MPa]	(aproximated)
3	Mooney-Rivlin (*)	$c_1 = 0.66$, $c_2 = 4.5$ [MPa]	(aproximated)
4	Yeoh	$c_1 = 1.25$, $c_2 = 2.25$ [MPa]	[7]
5	Mooney-Rivlin	$c_1 = 0.66$, $c_2 = 0.25$ [MPa]	[25]
6	Neo-Hookean	$c_1 = 0.67$ [MPa]	[25]

These different values shows difficult problem with determination of properties. Its strength depends on the measurements method. The case 2 and 3 in Table 1 is focused on two cases of nonlinear, hiperelastics models of cartilage. The parameters for definitions of these models were selected based on stress – strain curve presented by the Danso [24]. The case 4 defines the hiperelastic material described by the Robinson [7]. The Fig. 3 presents relationship between stress and strain for all 6 selected cartilage models. The cases 5 and 6 are characterized by a too much lesser stiffness like in other models.

The Fig. 3 presents stress-strain relationship for particular models of articular cartilage. The curves presented on the graph are different at the beginning phase of deformation. The model 2 is characterized by the greater stiffness in comparison to models 3 and 4. In result for the strain equal about 0.75 mm/mm

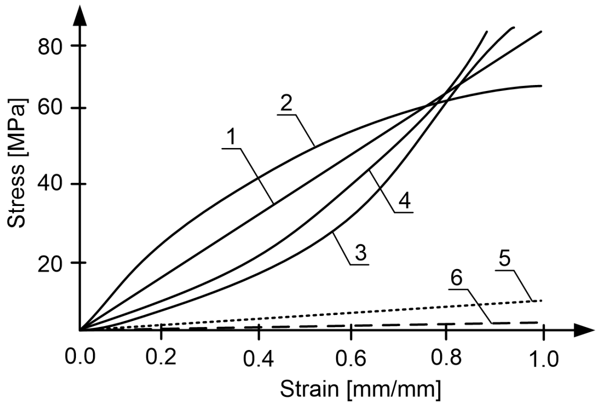

Fig. 3. The relation strain-stress for each model of articular cartilage: 1 – isotropy model, 2 – Noe-Hookean* model, 3 – Mooney-Rivlin model*, 4 – Yeoh model, 5 – Mooney-Rivlin model, 6 – Noe-Hookean model.

the stress for 1, 2, 3, 4 models have similar value. Finally, for our investigation, the cartilage structure was assumed as the one layer with properties presented in the Table 1.

3. Results

In this study the aim of numerical experiments were defined around three aspects. The first aspect is focused on the energy transmission in muscle-bone structures. The role of articular cartilage was determined as the damping component causing the decrease of reaction force in biomechanical chain of the lower extremity. It was realized by the investigation of influence the cartilage properties on reaction force in the support. The second aspect is the study of a relationship between a contact area and a strain energy calculated for tibia bone during loading. In result of these calculations the behaviour of joint after preliminary loaded was analysed. This preload has led to some changes of the conditions of contact between the articular surfaces. The third aspect is concentrated on the role of the cartilage thickness.

The changes of distance between bones in an articular joint lead to the change of thickness of cartilage and a synovial film. In result, the investigation of thickness changes can give a response about the mechanism of damping in an articular joint. Based on changes of reaction force and also after analysis the change of strain energy in the tibia, can be used to the definition of the internal force in the extremity generating during impact loading. According to the previous studies, the value of force applied axially to the tibia [29]. This data can be used to determine the probability of a damage generated in bone structures. Based on these investigations the value of load force was selected. The criterion for this choice was 50% of probability of injury in the lower extremity during axial load [34].

3.1. Reaction force analysis

The numerical experiments of supporting and loading were done with an assumption that the load force is generated by dislocation of a talus along biomechanical axis of the lower extremity. This solution lead to the reliability that the load was the same for all analysed cases.

The Fig. 4 presents the values of reaction force measured on the cartilage surface in the proximal head of the tibia in the place of the contact with femur in the knee. The changes of the response force values are indicated to determine a part of energy which has been absorbed.

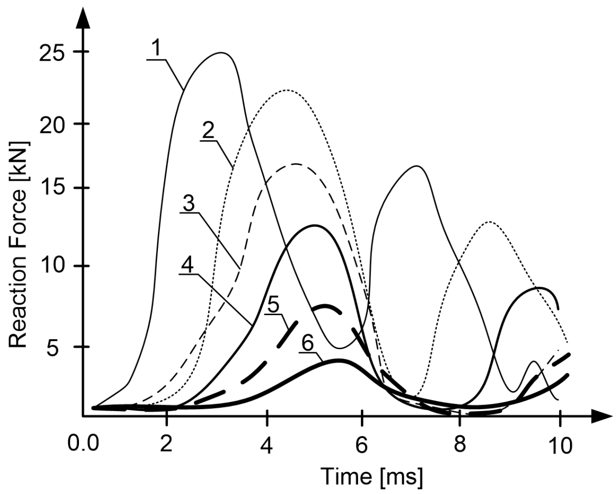

FIG. 4. The reaction force for particular material model of cartilage.

3.2. Contact analysis

The contact area between joint surfaces depends on the passed force. The amount of energy transmitted by this contact has influenced the density of the energy stream. In order to calculate this energy the internal energy of strain was used.

The changes of contact were realized based on simulation process that consists of two steps. The first step was defined by the approximation of the possible load resulting from the body weight and additionally from other sources like inertial forces. In practice the value of the load was assumed as 100 kG, 50 kG and 25 kG.

The second step of this process comes after the preload. The model is powered by a dynamic inertia force which is generated during the upwards movement of talus along the biomechanical axis of a leg. The kinematic parameters are formed as the peak movement with the velocity of 7 m/s. The velocity was selected as a typical strong load of a leg during the explosion of IED charge in military vehicles [10].

The Fig. 5 shows the energy value generated inside the tibia under loading. Three cases of contact area are presented on the graph, for which the amount of energy is similar. The same portion of energy is transmitted by the small or large area. In result the density of energy is changed. For the case 3 the stresses are the highest. This situation can lead to a damage of the cartilage surface.

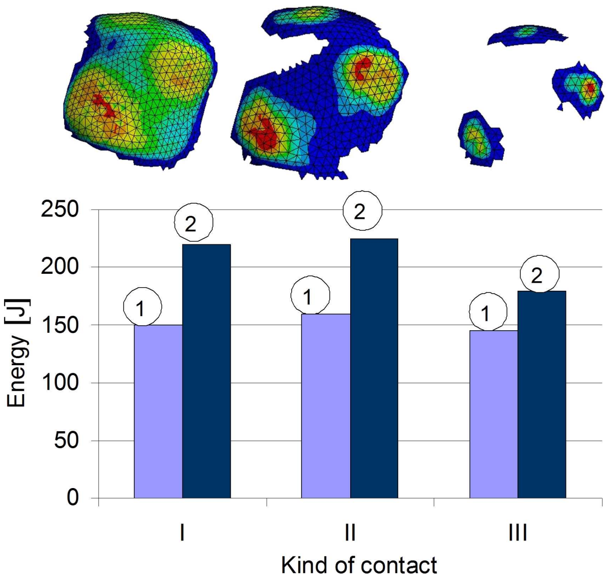

Fig. 5. Energy for different contact area.

3.3. Thickness analysis

The third part of investigations was focused on the influence of cartilage thickness on the damping energy in the tibiotalar joint. The thickness values in these calculations are chosen in 3–5 mm range. In result the thickness of the components is defined by the cartilage layer on the both bones in joint and synovial capsule. The thickness corresponds to the average thickness in healthy joints of adults [23].

The Fig. 6 presents the relationship between a change of thickness and an energy accumulated in tibia bone for two selected material models. For the

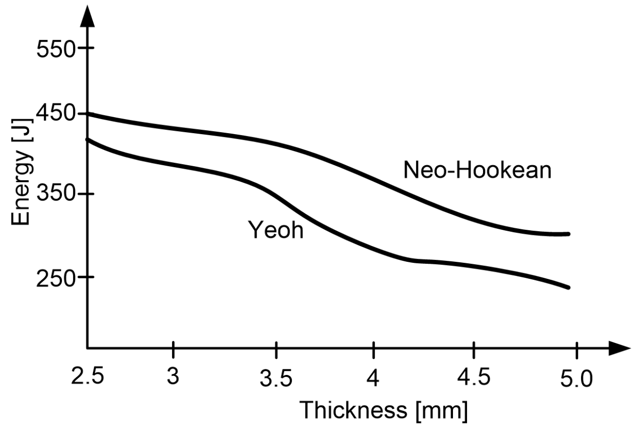

FIG. 6. Relationship between cartilage thickness and deformation energy in tibia.

Neo-Hookean model of cartilage material the results show that the energy is characterized by a lower absorption in comparison to Yeoh model. The Neo-Hookean model is more deformed under less stress. In consequence, the energy need to deform is lower and more energy is transmitted to tibia. The Yeoh model is characterized by higher stiffness and in result the energy is more dissipated.

4. Discussion

For the impact loading of lower extremity the probability of injury is defined according to axial force occurring inside of the extremity [29]. The empirical study shows, that the 50% probability of injury in the lower leg may occur for 6–8 kN of load force. In result of these experiments it has not been clear what is the reason of big force differences which is needed to the destruction.

The results have shown that the articular cartilage has an important role in shaping the effort of bone structure. In many works the role of a cartilage layer in energy transmission is completely ignored [30, 31]. The results appeared that the cartilage has a significant role in damping energy and creating dangerous stresses in the hard and soft tissues. The contact area in a tibiotalar joint is not an important condition for the energy absorption by a joint. Some small changes were observed for the different cartilage thickness. The calculations were done in ANSYS software for mesh from over 523 000 elements from which about 350 000 were used for modeling of a tibiotalar joint. The high density of the mesh provided to the accurate calculations of the deformations and stresses in the cartilages.

In order to validate the model, the result of modeling was compared to the clinical information about effects of axial impact load in a shank. In the literature there are numerous clinical situations in which the axial load leads to the bone fractures in both fibula and tibia.

The Fig. 7a shows the stress map for tibia and fibula during axial load. The distribution of the axial loading in the model resulted in the concentration of stresses in a diaphysis of tibia. The stresses over the ultimate value caused the creation of damages in the tibia bone. After the loss of stability by the tibia, the loading is transferred by the fibula. As a result, the fibula is also destroyed. The example of this process is shown on CT picture (Fig. 7b). The results of analysis indicate that the cartilage has an important role in energy transmission by the extremity. For the numerical models without cartilage [30, 31] the investigation of resistance of extremity on the impact load is not enough because the damping properties of the cartilage change the behaviour of all models and provide to the less values of the forces. To understand it better, the process of energy distribution of the numerical models must contain such elements as: cartilages layers, synovial capsules, ligaments and muscles.

a) b)

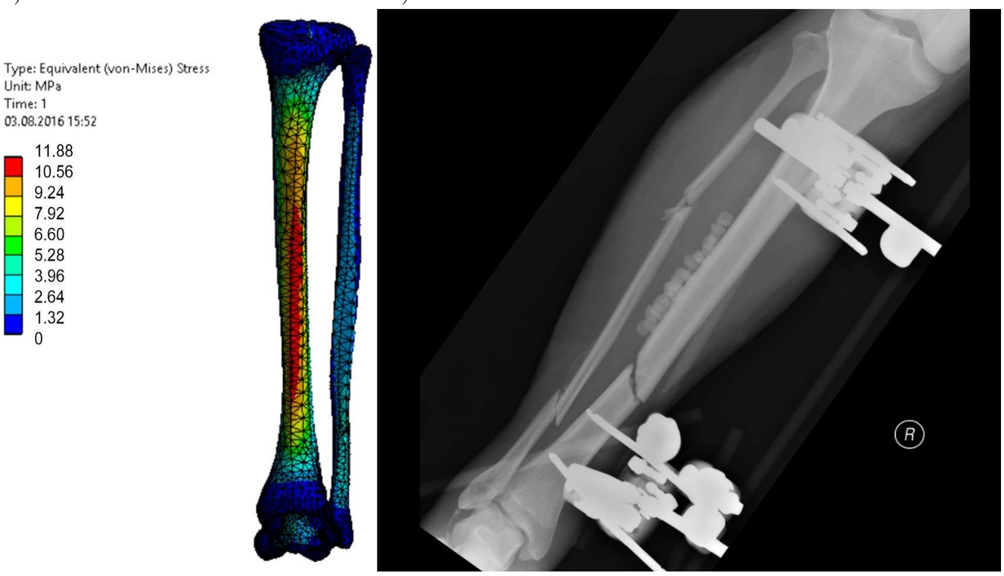

Fig. 7. a) Stress distribution under axial load, b) CT image for the lower extremity after damage.

5. Conclusions

The simulations carried out in this paper lead to the conclusion that the model had a different behaviour for different cartilage properties. For the cartilage with a higher stiffness (about 100 MPa) the reaction force is very high.

This situation can be cause a damage of bones in a leg. For the cartilages with less stiffness the result shows that the reaction force is clearly less. During the investigation on the cadavers or dummies the destroyed force is defined in the range 8–12 kN. Taking into account the results from this study the conclusion about the dangerous loading of lower extremity is that the cartilage layer in the cadaver leg has a significant higher stiffness. Due to the fact that the important role in mechanical properties of cartilage material is a content of the water, the conclusion is that the preparates form cadavers having dried the cartilage.

The presented results were realized for constant properties of the bone to focus on the function of the soft tissues. The influence of contact area on energy transmission was examined with an assumption that this contact between cartilage layers of both bones is created during preliminary load. The energy cumulated in the tibia is similar for different contact areas, but the stress in the cartilage for the smallest contact area was very high and equal about 120 MPa. The ultimate stress for cartilage is defined about 27 MPa [32, 33] and usually is defined by the yield strength. This level of stress in cartilage is dangerous because it causes the risk of permanent damage of the cartilage surface, what is difficult to recover.

References

1. Hunziker E.B., *Articular cartilage repair: basic science and clinical progress. A review of the current status and prospects*, Osteoarthritis and Cartilage, **10**(6): 432–463, 2002, doi: 10.1053/joca.2002.0801.
2. Li G., Wan L., Kozanek M., *Determination of real-time in-vivo cartilage contact deformation in the ankle joint*, Journal of Biomechanics, **41**(1): 128–136, 2008, doi: 10.1016/j.jbiomech.2007.07.006.
3. Mow V.C., Kuei S.C., Lai W.M., Armstrong C.G., *Biphasic creep and stress relaxation of articular cartilage in compression? Theory and experiments*, Journal of Biomechanical Engineering, **102**(1): 73–84, 1980, doi: 10.1115/1.3138202.
4. Bischof J.E. *et al.*, *In vivo cartilage contact strains in patients with lateral ankle instability*, Journal of Biomechanics, **43**(13): 2561–2566, 2010, doi: 10.1016/j.jbiomech.2010.05.013,
5. Akiyama K. *et al.*, *Three-dimensional distribution of articular cartilage thickness in the elderly cadaveric acetabulum: a new method using three-dimensional digitizer and CT*, Osteoarthritis and Cartilage, **18**(6): 795–802, 2010, doi: 10.1016/j.joca.2010.03.007.
6. Anderson D.D. *et al.*, *Physical validation of a patient-specific contact finite element model of the ankle*, Journal of Biomechanics, **40**(8): 1662–1669, 2007, doi: 10.1016/j.jbiomech.2007.01.024.
7. Robinson L.D. *et al.*, *Mechanical properties of normal and osteoarthritic human articular cartilage*, Journal of the Mechanical Behavior of Biomedical Materials, **61**: 96–109, 2016, doi: 10.1016/j.jmbbm.2016.01.015.

8. Garcia-Aznar J.M. *et al.*, *Load transfer mechanism for different metatarsal geometries: a finite element study*, Journal of Biomechanical Engineering, **131**(02): 021011–021011-7, 2009, doi: 10.1115/1.3005174.

9. Melińska A., Czamara A., Szuba Ł, Będziński R., *Biomechanical characteristics of the jump down of healthy subjects and patients with knee injuries*, Acta of Bioengineering and Biomechanics, **17**(2): 111–120, 2015, doi: 10.5277/ABB-00208-2014-04.

10. Klekiel T., *Biomechanical analysis of lower limb of soldiers in vehicle under high dynamic load from blast event*, Series on Biomechanics, **29**(2–3): 14–30, 2015.

11. Bailey A.M., Christopher J.J., Salzar R.S., Brozoski F., *Comparison of Hybrid-III and postmortem human surrogate response to simulated underbody blast loading*, Journal of Biomechanical Engineering, **137**(5): 051009–051009-10, 2015, doi: 10.1115/1.4029981.

12. Niu W. *et al.*, *Effects of bone Young's modulus on finite element analysis in the lateral ankle biomechanics*, Applied Bionics and Biomechanics, **10**(4): 189–195, 2013, doi: 10.3233/ABB-140085.

13. Connor C.J., Nabhani F., *Biomechanical evaluation of external ankle arthrodesis contact area and pressure distribution*, Journal of Materials Processing Technology, **153–154**: 174–178, 2004, doi: 10.1016/j.jmatprotec.2004.04.140.

14. Bayod J, Becerro-de-Bengoa-Vallejo R., Losa-Iglesias M.E., Doblaré M., *Mechanical stress redistribution in the calcaneus after autologous bone harvesting*, Journal of Biomechanics, **45**(7): 1219–1226, 2012, doi: 10.1016/j.jbiomech.2012.01.043.

15. Beddoes M.C., Whitehouse R.M., Briscoe H.W., Su B., *Hydrogels as a replacement material for damaged articular hyaline cartilage*, Materials, **9**(6): 443, 2016, doi:10.3390/ma9060443.

16. Rho J-Y., Kuhn-Spearing L., Zioupos P., *Mechanical properties and the hierarchical structure of bone*, Medical Engineering & Physics, **20**(2): 92–102, 1998, doi: 10.1016/S1350-4533(98)00007-1.

17. Xu C. *et al.*, *Biomechanical evaluation of tenodesis reconstruction in ankle with deltoid ligament deficiency: a finite element analysis*, Knee Surgery, Sports Traumatology, Arthroscopy, 20(12): 1854–1862, 2012, doi: 10.1007/s00167-011-1762-z.

18. Gannon A.R. *et al.*, *The changing role of the superficial region in determining the dynamic compressive properties of articular cartilage during postnatal development*, Osteoarthritis and Cartilage, **23**(6): 975-984, 2016, doi: 10.1016/j.joca.2015.02.003.

19. Klekiel T., Będziński R., *Finite element analysis of large deformation of articular cartilage in upper ankle joint of occupant in military vehicles during explosion,* Archives of Metallurgy and Materials, **60**(3): 2115–2121, 2015, doi: 10.1515/amm-2015-0356.

20. Shin J., Yue N., Untaroiu C.D., *A finite element model of the foot and ankle for automotive impact applications*, Annals of Biomedical Engineering, **40**(12): 2519–2531, 2012, doi: 10.1007/s10439-012-0607-3.

21. Suresh M. *et al.*, *Finite element evaluation of human body response to vertical impulse loading*, [in:] Proceedings of the 10th World Congress on Computational Mechanics, São Paulo: Blucher, 2014, Blucher Mechanical Engineering Proceedings, **1**(1): 1809-1818, 2014, doi: 10.5151/meceng-wccm2012-18555.

22. Ramlee M.H., Kadir M.R.A., Murali M.R., Kamarul T., *Biomechanical evaluation of two commonly used external fixators in the treatment of open subtalar dislocation – a finite element analysis*, Medical Engineering & Physics, **36**(10): 1358–1366, 2014, doi: 10.1016/j.medengphy.2014.07.001.

23. , *et al.*, *Quantification of ankle articular cartilage topography and thickness using a high resolution stereophotography system*, Osteoarthritis and Cartilage, **15**(2): 205–211, 2007, doi: 10.1016/j.joca.2006.07.008.

24. Danso E., Honkanen J.T.J., Saarakkala S., Korhonen K.R., *Comparison of non-linear mechanical properties of bovine articular cartilage and meniscus*, Journal of Biomechanics, **47**(1): 200–206, 2014, doi: 10.1016/j.jbiomech.2013.09.015.

25. Butz D.K., Chan D.D., Nauman A.E., Neu C.P., *Stress distributions and material properties determined in articular cartilage from MRI-based finite strains*, Journal of Biomechanics, **44**(15): 2667–2672, 2011, doi: 10.1016/j.jbiomech.2011.08.005.

26. Venturanto C. *et al.*, *Investigation of the biomechanical behaviour of articular cartilage in hindfoot joints*, Acta of Bioengineering and Biomechanics, **16**(2): 57–65, 2014, doi: 10.5277/abb140207.

27. Safari M. *et al.*, *Clinical assessment of rheumatic diseases using viscoelastic parameters for synovial fluid*, Biorheology, **27**(5): 659–674, 1990.

28. Ozen M., Sayman O., Havitcioglu H., *Modeling and stress analyses of a normal foot-ankle and a prosthetic foot-ankle complex*, Acta of Bioengineering and Biomechanics, **15**(3): 19–27, 2013.

29. Nilakantan G., Tabiei A., *Computational assessment of occupant injury caused by mine blasts underneath infantry vehicles*, International Journal of Vehicle Structures & Systems, **1**(1–3): 50–58, 2009, doi: 10.4273/ijvss.1.1-3.07.

30. Dong L. *et al.*, *Blast effect on the lower extremities and its mitigation: a computational study*, Journal of the Mechanical Behavior of Biomedical Materials, **28**: 111–124, 2013, doi: 10.1016/j.jmbbm.2013.07.010.

31. Kraft R.H., Lynch M.L., Vogel E.W., *Computational failure modeling of lower extremities*, Raport NATO RTO-MP-HFM-207, 2012.

32. Untaroiu C.D., Yue N., Shin J., *A finite element model of the lower limb for simulating automotive impacts*, Annals of Biomedical Engineering, **41**(3): 513–526, 2013, doi: 10.1007/s10439-012-0687-0.

33. Horst D.V.J.M., Simms K.C., Maasdam V.R., Leerdam C.J.P., *Occupant lower leg injury assessment in landmine detonations under a vehicle*, Michael D. Gilchrist [Ed.], IUTAM Proceedings on Impact Biomechanics: From Fundamental Insights to Applications, pp. 41–49, 2005, Springer.

34. Yoganandan N. *et al.*, *Dynamic axial tolerance of the human foot-ankle complex*, R. H., Society of Automotive Engineers, Paper 962426, Warrendale, PA., 1996.

Received October 25, 2016; accepted version December 15, 2016.